Eur Biophys J (1993) 22:301–307

European Biophysics Journal

Electrostatic interactions in gramicidin channels

Three-dielectric model

G. Martinez, M. Sancho

Facultad de Física, Departamento de Física Aplicada III, Universidad Complutense, E-28040 Madrid, Spain

Received: 19 October 1992 / Accepted in revised form: 18 May 1993

Abstract. A model based on the solution of the electrostatic potential for a geometry of three dielectric regions associated with a gramicidin A channel (GA) is presented. The model includes a cylindrical dielectric layer to represent the peptide backbone and dipole rings to account for dipolar side chains. Image potential and dipolar contributions for different orientations and positions along the channel are analyzed. The conductance of GA and two analogues obtained by substituting the amino acid at position 1 are studied. The numerical simulation reproduces experimental results (Barrett et al. 1986, Biophys J 49, 673–686) and supports the idea that electrostatic dipole–ion interactions are of primary importance in gramicidin channel function.

Key words: Ion-channel interaction – Gramicidin – Electrostatic model – Channel conductance – Residue substitution

Introduction

The commonly accepted structure for a great variety of ion channels is that of an aqueous pore. The protein which forms the pore walls represents an envelope with favorable interactions to compensate for the dehydration experienced by the ion. From an electrostatic point of view, the protein may be considered as a polar medium which reduces the image energy of the ion, due to the low permittivity of the membrane.

One of the most widely studied pore formers is the gramicidin *A* molecule; it is a polypeptide with the following amino acid sequence: formyl-L-Val^1-Gly^2-L-Ala^3-D-Leu^4-L-Ala^5-D-Val^6-L-Val^7-D-Val^8-L-Trp^9-D-Leu^{10}-L-Trp^{11}-D-Leu^{12}-L-Trp^{13}-D-Leu^{14}-L-Trp^{15}-ethanolamine. The alternating L-D sequence allows gramicidin to form N-N terminal dimers of β (6.3) helices, providing a central pore lined with the polar peptide groups, while side chains are situated some 5–10 Å from the lumen.

Correspondence to: G. Martínez

Electrostatic calculations of the energetics of an ion inside a channel focus on the image energy, which seems to be the main limiting factor to the passage of the ion (Jordan 1986). They provide a macroscopic picture of molecular events and thus cannot explain ion-specific features. Nevertheless, they constitute a useful tool for interpreting experimental results in terms of the influence of structural parameters on the channel function.

Different mathematical schemes for determining potentials in a geometry simulating a channel have been proposed (Levitt 1978; Jordan 1981, 1982; Partenskii et al. 1991). In a previous study (Sancho and Martínez 1991), we presented a method which allows an accurate calculation of the potential distribution in a gramicidin-like channel and incorporates the dipolar contributions due to the side chains. There is experimental evidence of the important role played by these polar groups (Heitz et al. 1982; Barrett et al. 1986; Andersen et al. 1987; Becker et al. 1991; Fonseca et al. 1992) and that their effects arise from direct electrostatic interactions rather than from inductive shifts in electron densities or steric alterations (Koeppe et al. 1990). In this article we extend the formulation, considering an additional dielectric domain to account for the electric polarization of the polypeptide backbone. This gives a more realistic simulation which uses the physical radius instead of an effective electrical radius and represents better the effect of the polar side chains on the ion, which is modified by the protein polarization. The electrical radius, present in most two-dielectric calculations, is an undesirable parameter because it depends on the ion position (Monoi 1991).

The ion energy along the channel, combined with the electrodiffusion equation, gives the flux for a given bulk concentration and applied voltage. Following this procedure we analyze the experimental characteristics obtained by Barrett et al. (1986) using modified gramicidens in which residue Val at position 1 was substituted by others with different polarity. We discuss the results and show that they can be explained by long range electrostatic effects in which both the magnitude and orientation of dipole moments are of importance.

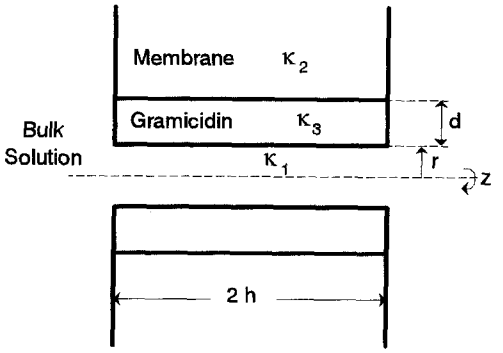

Fig. 1. Cross sectional diagram of the cylindrical system used in the simulation of a GA channel. The bulk water and the pore region have the same dielectric constant $\varkappa_1$, the membrane is characterized by $\varkappa_2$ and the pore wall by $\varkappa_3$

Theory

Model parameters

In our macroscopic model, we choose a three-dielectric system to represent the channel incorporated into a lipid membrane (Fig. 1): the exterior aqueous medium and the water within the pore, with dielectric constant $\varkappa_1 = \varepsilon_1/\varepsilon_0$; the membrane, characterized by $\varkappa_2$; and the backbone peptide, characterized by $\varkappa_3$. The configuration has rotational symmetry about the channel axis, and the origin is put at the center of the pore. The form and dimensions are taken as those of the gramicidin, whose structure is well known, and for which there is an abundance of experimental results to compare with the theoretical predictions. Parameters accepted in the literature are (Jordan 1982; Boni et al. 1986; Monoi 1991): r = 2.1 Å, d = 2.8 Å, h = 12.5 Å, $\varkappa_1 = 80$, $\varkappa_2 = 2$ and $\varkappa_3 = 10$. The ion is treated as a point charge, restricted to movement along the channel axis. The polar nature of some side chains is represented by dipolar rings coaxial with the pore, with radii slightly greater than that of the region $\varkappa_3$; the hypothesis of dipolar moment distributed over rings is necessary to keep the rotational symmetry, and is a reasonable approximation to a distribution of dipoles along the helical structure. Also, we have ignored ionic charge effects in the aqueous exterior, this may be considered as a valid assumption for narrow pores and ionic strengths up to approximately 0.1 M (Jordan et al. 1989).

Calculation of the electrostatic potential

The classical approach to the computation of electrostatic fields in media which involve proteins and various phases consists of the application – in discrete form – of Poisson's equation (Warwicker and Watson 1982), with appropriate boundary conditions. If the problem is represented by linear dielectric media, it is advantageous to use an integral formulation (Martínez and Sancho 1991). This treatment avoids the calculation of numerical derivatives, which are computationally inaccurate, bypasses the problem of dealing with the singularities due to the presence of corners, and, in addition, reduces the effective dimensions of the problem by considering elements only over the surface of the contours. In our formulation, the boundary conditions are explicitly incorporated, and do not introduce equivalent charges as in other approaches.

For the geometry of Fig. 1, the following system of integral equations can be deduced (Martínez and Sancho 1991)

$$\phi(\mathbf{r}) = \frac{2\varkappa_1}{\varkappa_I + \varkappa_J}\phi_S(\mathbf{r}) + \frac{1}{2\pi\varepsilon_O(\varkappa_I + \varkappa_J)}\int_{S_C}\frac{\sigma(r')}{R}\mathrm{d}s - \frac{1}{2\pi(\varkappa_I + \varkappa_J)}\sum_{S_{LM}}(\varkappa_L - \varkappa_M)\int_{S_{LM}}\phi(\mathbf{r}')\frac{\partial}{\partial n'}\left(\frac{1}{R}\right)\mathrm{d}s',\ \mathbf{r}\ \varepsilon\ S_{IJ} \quad (1)$$

$$\phi(\mathbf{r}) = \text{const.} = \phi_S(\mathbf{r}) + \frac{1}{4\pi\varepsilon_1}\int_{S_C}\frac{\sigma(\mathbf{r})}{R}\mathrm{d}s' - \frac{1}{4\pi\varkappa_1}\sum_{S_{LM}}(\varkappa_L - \varkappa_M)\times\int_{S_{LM}}\phi(\mathbf{r})\frac{\partial}{\partial n'}\left(\frac{1}{R}\right)\mathrm{d}s,\ \mathbf{r}\ \varepsilon\ S_C$$

in contact with the dielectric ε_1 (2)

where $R = |\mathbf{r}-\mathbf{r}'|$, S_C represents the electrode surfaces, S_{IJ} is the interface between the media of dielectric constants $\varkappa_I$ and $\varkappa_J$; ϕ_S is the potential produced by the space sources assumed to be in medium 1.

In the last terms, n' is the normal to the interface S_{LM} taken from the medium L to the medium M.

In Eqs. (1) and (2) the three terms of the right-hand side represent the contribution of the ion and dipole, surface charges on the electrodes and polarization charges on the interfaces, respectively. Boundary conditions are incorporated through Eq. (2) with the potential given on the electrodes. The formulation does not enclose singularities as $\phi(\mathbf{r})$ is a continuous variable.

Numerical technique

Harrington (1968) provided a treatment for the numerical solution of linear operator problems, the method of moments. In this technique, the discretisation is performed by expanding the unknowns in a series of basis functions and projecting the equations by means of an inner product with some defined test functions.

We have divided the boundaries into a set of small subareas. Constant values of ϕ or σ are assumed on them, and the equations are applied to representative points of each sub-area (usually the midpoint). This is equivalent to the selection of pulse and Dirac delta as basis and test functions respectively. We have proved that this version of the method allows an efficient and very precise solution for the potential in continuum models (Algora et al. 1987; Martínez and Sancho 1990).

According to these considerations, let the index j go from 1 to k to account for dielectric subareas, and from $k+1$ to n for conducting ones. After applying the technique, Eqs. (1) and (2) are converted into the following

set of algebraic equations

$$\phi_i = \frac{2\varkappa_1}{\varkappa_I + \varkappa_J}\phi_S(\mathbf{r}_i) + \sum_{j=1}^{k} A_{ij}\,\phi_j + \sum_{j=k+1}^{n} B_{ij}\sigma_j,\ i = 1,k \quad (3)$$

$$\phi_i = \text{const.} = \phi_S(\mathbf{r}_i) + \sum_{j=1}^{k} C_{ij}\,\phi_j = \sum_{j=k+1}^{n} D_{ij}\,\sigma_j,$$

$$i = k+1,n \quad (4)$$

corresponding to representative points on the dielectric and on the conductor surfaces, respectively. In our geometry of Fig. 1, the external radius of the membrane surface and the radii of two electrodes set at $\pm$ 6 h, are taken as 12 h; a further increase does not appreciably modify the results. The contours are divided into annular or cylindrical sub-areas and, unless otherwise stated, the total number of dielectric and conducting sub-elements used are 134 and 24, respectively.

One of the main advantages of this version is that coefficients A_{ij}, B_{ij}, C_{ij}, D_{ij} can be evaluated by means of analytical expressions for the type of sub-areas in consideration (for details, see Martínez and Sancho 1991). Expressions for the contribution to ϕ_S of dipolar rings are given in the Appendix. Taking advantage of the symmetry of the configuration with respect to the $z = 0$ plane, the number of matrix coefficients to be computed is halved. To minimize round of errors, the 158×158 matrix is inverted by partitioning into four sub-matrices, using Crout reduction for each partial inversion. The computation is performed with double precision (16 digits).

Error of the method

As we outlined, the first step in the solution by the moment method is the division of the contour of the geometry into sub-elements. Errors in the calculated magnitudes are mainly dependent on the way this division is performed. The simplest possibility is to make a uniform discretisation, with all the sub-areas having the same width, but this is rather inefficient because of the high number of sub-areas required. As the unknowns are assumed to be constant for each sub-area, a division closer to the physical picture is much more efficient. Thus, a uniform width is used in regions where these functions vary slowly, while progressively smaller sub-areas are distributed near the edges, corners or spatial sources, where rapid variations are expected.

We have analyzed errors in the boundary conditions using three different tests: *1)* Points on the conductor surfaces must be at the polarization potential ($\pm V_0$); *2)* The potential is a continuous function in crossing the boundary between two dielectric regions; *3)* "Refraction law" for the normal component of the electric field holds at this boundary phase ($\varepsilon_I E_{In} = \varepsilon_J E_{Jn}$).

Figure 2 gives the distribution of the relative error (%), found at points on the conductor (other than the representative points), as a function of the number of sub-elements n. We see that, in general, the error diminishes as n increases; however, at some points the behavior is reserved. This is due in part to randomness with which

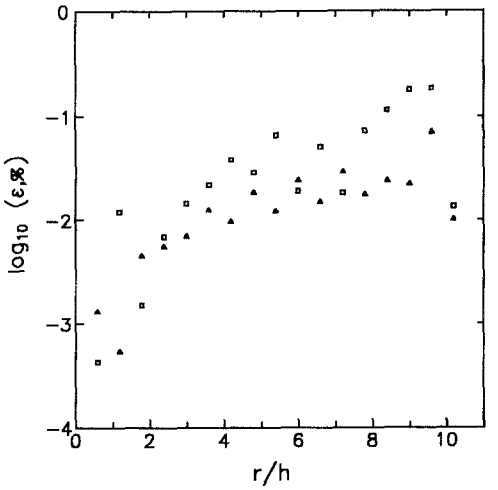

Fig. 2. Relative error for calculated potential on the surface of an electrode, for two different divisions of the geometry of Fig. 1. *Open squares:* $n = 130$; *full triangels:* $n = 158$

errors in the calculations are added; besides, if the point is near the edge of a sub-area, one of the elliptic integrals of the first kind involved in the computation of the potential will have a modulus near unity which can lead to an imprecise result. In both cases, the maximum error found near the axis ($r \leq h$), was less than 0.002%.

For the other two tests, we have checked that the interface conditions hold up to 6 significant digits in the case of the potential extrapolated from both sides of a representative point and up to 3 significant digits for the normal component of the vector $\varepsilon\mathbf{E}$.

The previous results give reliability to the computation but do not provide an error figure at an arbitrary point of the region of interest. The main source of error in the method is the substitution of the continuous distribution of charges and potential by a discrete one. This produces an error which can be important near a sub-element but decreases rapidly when the point separates from the interface and the distribution can be viewed as continuous. For points along the axis of the channel, comparison with potentials calculated by other methods and asymptotic results for an infinite channel, allows an estimation of the net error lower than 0.1%.

Flux equations

Given the smooth nature of the energy profiles that we obtain, with a barrier about 20 Å wide, a continuum approach to the ion translocation seems the most appropriate. If the channel is occupied by few ions, the electrodiffusion equations are still valid but they contain the probability density for the ion at a given position, instead of concentration (Levitt 1986; Gates et al. 1989). Assuming that the ends of the channel are at equilibrium with the bulk concentrations, the final solution reduces to the classical Nernst-Planck equation; thus the ion flux is given by

$$J = \mathrm{DA}\frac{C_1 e^{v_1} - C_2 e^{v_2}}{\int e^{v}\,\mathrm{d}z} \quad (5)$$

where $v = e\phi/kT$; D is the diffusion coefficient and A the area available for the ion; 1 and 2 are the extreme positions of the ion trajectory. The value DA, obtained by fitting to experimental currents in GA is 8×10^{-28} $m^4 s^{-1}$. This quantity would represent a mean value of the product of the area and the diffusion coefficient along the ion trajectory between the electrodes, and is reasonable given the uncertainity in these parameters (The product DA for the diffusion coefficient of Cs^+ in water and the area corresponding to the physical radius of 2.1 Å is 2.8×10^{-28} $m^4 s^{-1}$).

Results and discussion

The energy profiles of the ion along the channel have been obtained as the sum of three terms:

$$U = e(1/2\phi_i + \phi_v + \phi_d)$$

where the first contribution is the image energy due to the dielectric polarization induced by the ion; the second is the energy due to the applied voltage; and the third represents the interaction with the dipolar moments of the side chains, assuming that they have a specific effect not included in the permittivity ε_3. Each of these terms are computed independently, using equations similar to Eq. (4); for the determination of ϕ_i and ϕ_d the electrodes are set at *0* V.

We have first studied the variation of the image energy as a function of the most relevant parameters. Figures 3 and 4 show these profiles for different values of $\varkappa_3$ and d. The influence of the width of the region assigned to the channel wall is particularly noticeable. In what follows, we will use $\varkappa_3 = 10$ and $d = 2.8$ Å, which are values used in the literature and give barriers of an appropriate magnitude.

In addition to the facilitating effect of the central solvation path, the side chains play an essential role in the ion permeation. The channel conductance is substantially altered when certain replacements of single amino acids are performed, even though the side chains do not directly contact the permeating ion but rather are separated by 5–10 Å from the pore. In a previous study (Sancho and Martínez 1991), and using a two-dielectric model, we have done a general analysis of the influence of the dipolar interactions and showed that the observed changes in conductance can be explained as a long range electrostatic effect. The more realistic three-dielectric model corroborates the previous predictions. Figure 5 depicts the main characteristics of the effect of two dipolar rings, simulating the behavior of symmetric side chains in the gramicidin dimer. The resulting potential reflects the direct dipole contribution (the ϕ_S term) plus that due to polarization charges induced at the interfaces of the pore wall and membrane. The last quantity is of great influence when the dipolar rings are situated near the pore mouths and makes the predictions quite different from what would be expected for an infinite channel. We see that the barrier reduction for positive radially oriented dipoles ($\vartheta = 90°$), is maximum at positions near the center reaching a value of ≈ 25 mV per Debye; while for positive axial dipoles

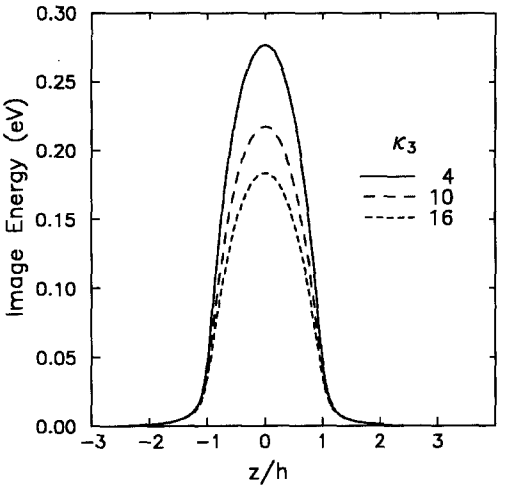

Fig. 3. Image energy profiles of the ion as a function of the dielectric constant $\varkappa_3$

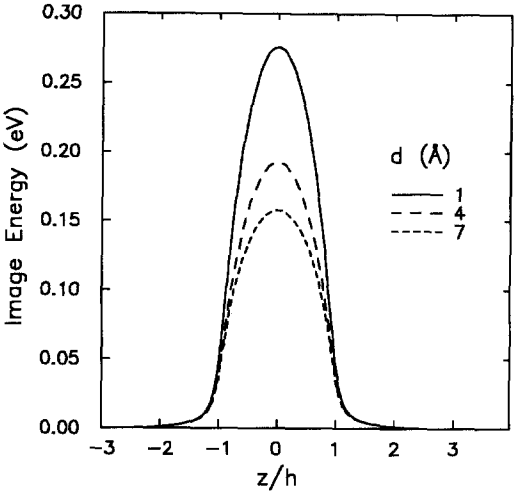

Fig. 4. Variation of the image energy profiles with the width of the pore wall region. The channel radius is kept at 2.1 Å

the external positions are more favorable, lowering the barrier ≈ 12 mV per Debye. At intermediate positions the greatest effect corresponds to orientations near 45°. (Axial positive moment means that the positive end of the dipole points toward the nearest end of the channel, and a radial positive dipole has its positive end pointing away from the axis).

In Fig. 6 we have studied the effect of the backbone dielectric constant on the potential produced by the dipole rings. The most negative value is represented as a function of $\varkappa_3$ and for three different axial positions of the rings. At high permittivities the potential increases with $\varkappa_3$, i.e. the dipoles are progressively screened; but the curves present minima for values of $\varkappa_3$ between 5 and 10. This noticeable behavior is due to the induced charges on the lateral backbone and membrane surfaces; we have verified that the minima disappear when the permittivity of medium 1 is lowered and, consequently, the lateral image charges are reduced.

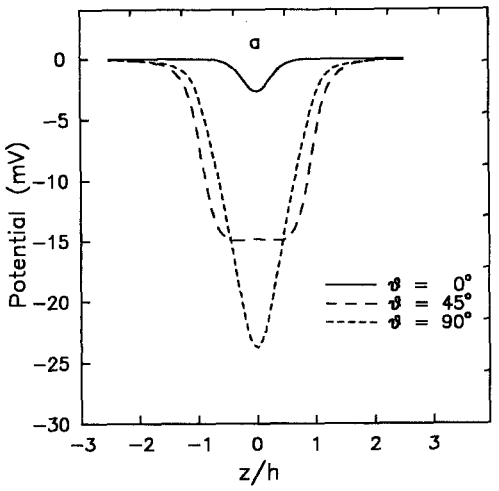

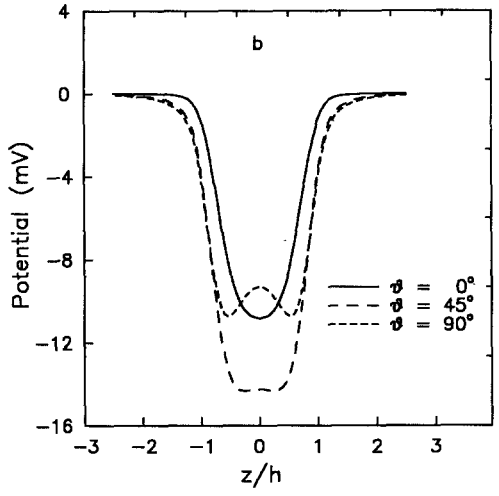

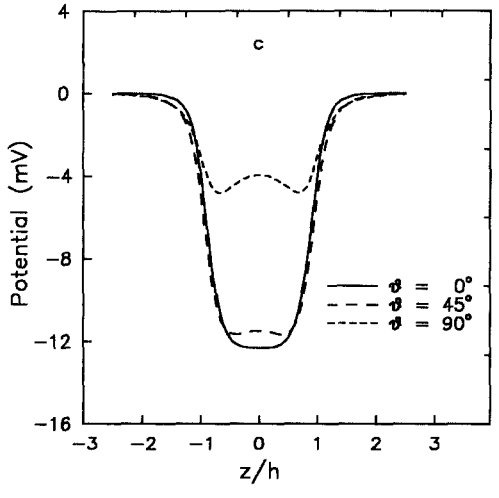

Fig. 5a–c. Potential created by two dipolar rings with $p = 1$ D and radii of 6 Å, for different values of the axial position and orientation. ϑ is the angle between the dipole moment and the z-axis in the right-hand side of the channel. The orientation of the left-hand side moment is symmetrical with respect to the plane $z = 0$. **a** $z = \pm 1$ Å; **b** $z = \pm 8.5$ Å; **c** $z = \pm 11.5$ Å

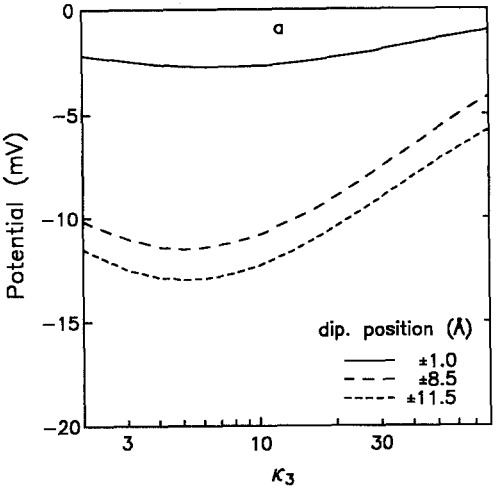

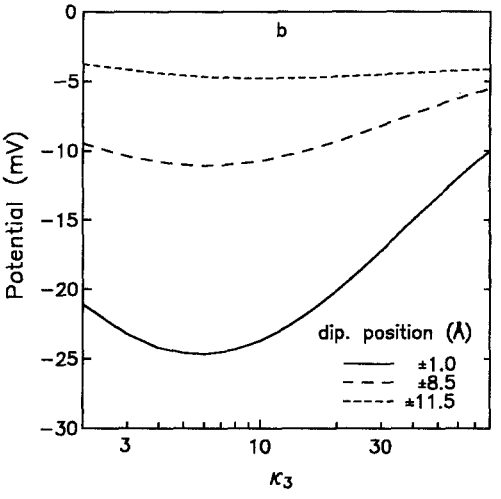

Fig. 6a, b. Effect of the backbone dielectric constant on the minimum value of the potential produced by a pair of dipole rings with radii of 6 Å and different axial positions $\pm z$ along the channel. **a** $p_r = 0$, $p_z = 1$ D; **b** $p_r = 1$ D, $p_z = 0$

As an example of the usefullness of the method, we have applied our model to the analysis of the substitution of amino acid residues at central positions in the gramicidin channel. Barrett et al. (1986), investigated the properties of GA analogues in which the NH_2 terminal valine was replaced by other amino acids whose side chains were essentially isosteric, but had different polarity (valine vs. trifluorovaline or hexafluorovaline). In our modeling this implies a variation in the magnitude and orientation of the dipolar rings simulating this contribution. The GA channel has been represented by two dipolar rings of radii 6 Å, with $p = 12$ D and at mean positions $z = \pm 8.5$ Å, reflecting the contribution of all polar residues excepting that of Val at position 1 (4 Trp and 3 Val in each monomer). The fit to experimental ionic currents gives a mean orientation $\vartheta = 71°$. In addition, this orientation agrees qualitatively with the behavior found in gramicidins with one Trp substituted by Phe. As the substitu-

Table 1. Variation of the single-channel current with the applied voltage in GA and two analogues. Upper quantities: experimental values taken from Fig. 4 of Barrett et al. (1986); lower quantities: numerical results obtained by fitting the orientation of the dipole moment of residue 1. The assigned values are: $p_r = 0.4$ D, $p_z = 0$ to valine; $p_r = -0.85$ D, $p_z = 0$ to trifluorovaline; and $p_r = -0.9$ D, $p_z = 1.5$ D to hexafluorovaline. The value DA is 8.10^{-28} m^{4}s^{-1} in all three cases

Applied potential (mV)	25	50	75	100
Valine-GA current (pA)	0.45	0.89	1.31	1.58
	0.46	0.89	1.29	1.63
Trifluorovaline-GA current (pA)	0.24	0.48	0.74	0.98
	0.24	0.49	0.76	1.05
Hexafluorovaline-GA current (pA)	0.26	0.52	0.75	0.98
	0.25	0.51	0.79	1.08

tion is moved from position 15 to 9 (toward the channel center) the measured conductance is lower (Becker et al. 1991, Table 1), which according to our model corresponds to the effect of mostly radially oriented dipoles.

The effect of valines at position 1 was simulated by two rings at $\pm$ 1 Å with $p = 0.4$ D and $\vartheta = 90°$. To mimic trifluorovaline-GA and hexafluorovaline-GA, a new fitting in the orientation was performed at position 1, taking dipole moments estimated from standard values of group moments (Barrett et al. 1986), i.e., 0.85 D and 1.75 D, respectively. The results of the theoretical predictions and the experimental values for GA and the two analogues, are contrasted in Table 1. The experimental values correspond to 0.1 M CsCl singel-channel current measurements, at low potentials where the effect of interfacial polarization – which has not been included in the model- is probably negligible (Andersen 1983). The important decrease of current from valine-GA to trifluorovaline-GA by a factor of almost 0.5 is explained by the change of dipole moment from 0.4 D oriented favorably to 0.85 D oriented unfavorably. The conductance of hexafluorovaline-GA is similar to that of trifluorovaline-GA even though its dipole moment is approximately double; this is achieved by assuming a large component along the z-axis, which has little effect on the energy barrier, as can be seen in Fig. 5a.

Recent research has questioned the modeling of narrow pores using an inner uniform dielectric medium of high permittivity. The simulation of permeation as a single-file shifting of the ion and a few water molecules along the pore demonstrates that the orientational mobility of water is greatly reduced, giving a low effective dielectric constant (Partenskii et al. 1991; Partenskii and Jordan 1992). However, the results are not conclusive yet, since they do not explain the observed high translocation rates. In any case, molecular dynamics calculations do not predict such dielectric saturation of water due to the presence of the ion, probably because of the compensating effect of flexible peptide groups (Jordan 1990). Our macroscopic approach with $\varkappa_1 = 80$ gives a basic energy profile in the absence of ion interaction with polar side chains, i.e., compatible with the observed conductance of gramicidin N. The same effect could possibly be obtained with a lower permittivity of the pore and by introducing dipoles to account in detail for flexible carbonyl effects, but this would increase the number of adjustable parameters and the complexity of the model. The important fact is that dipolar side chain contributions modify this basic barrier so as to produce the observed behaviour of GA channels and analogues.

Conclusions

We have presented a three-dielectric model which includes the main interactions responsible for the conductance in a gramicidin channel. The lowering of the high image energy due to the membrane is achieved through three factors: the solvation path constituted by the water inside the pore, a layer with dielectric constant intermediate between those of water and membrane, representing the pore former, and dipolar rings due to the polar side chains which are important in modulating the conduction. Compared to a previous two-dielectric model it has the advantage of considering more realistically the polarization effect of the protein instead of including it through an addition axially oriented dipolar ring. The dielectric shell produces a lowering of the image energy and, at the same time, shields the dipolar interactions. This permits the use of the physical radius instead of an effective one, and a reasonable distance for the dipole side chain contributions according to the accepted structure of the GA helix. The general conclusions about energy profiles of our two-dielectric model still hold, but there are quantitative differences in the relative contributions of axial and radial dipoles which have been summarized in Fig. 5. The radial orientation is still more effective in reducing the barrier for residue positions closer to the channel center; the axial one is dominating for dipoles close to the mouth; but now at intermediate positions (7–9 Å from the center), both orientations give similar contributions.

The energy maximum and the barrier shape are modulated by the magnitude and orientation of the dipolar moments and determine the conductance-voltage characteristics. The calculated curves $J-V$ are sensitive to variations of p and ϑ, thus allowing one to analyze the important modification of conductance observed in the experiments. We have studied alterations of the side chain at position 1. We have shown that the substitution of valine by triflurovaline or hexafluorovaline can be modeled using their estimated dipole moments with appropriate orientations. Although the model does not consider important aspects such as specific interactions which produce selective behavior or the partial dehydration of the ion at the channel entrance, its merit consists in showing the fundamental role of the macroscopic interactions, thus providing a method for analyzing the functional consequences of structural modifications. It would be interesting to check the validity of these conclusions with a molecular study using energy minimization of the structure or dynamics.

Appendix

The potential created by a uniform distribution of dipoles along a circumference, with a moment density v (C), can be calculated by superposing those of two oppositely charged rings. Alternatively, integration of elementary dipole contributions along the circumference can be used (Durand 1966). We must distinguish between two cases:

a) Distribution of dipoles with their moment parallel to the axis of the circumference

The resulting potential is in that case

$$V(\rho,z)=\frac{va}{\pi\varepsilon_0}\frac{z}{r_1^3}\frac{J_2(k)}{1-k^2}$$

where a is the radius of the circumference, J_2 is the complete elliptic integral of the second kind of modulus k, and

$$k=\frac{2(a\rho)^{1/2}}{r_1},\ r_1=[z^2+(a+\rho)^2]^{1/2}$$

For points on the axis, $k=0$, $J_2(k)=\pi/2$ and

$$V(0,z)=\frac{va}{2\varepsilon_0}\frac{z}{r_1^3}$$

b) Distribution of dipoles with radial moments

When the dipoles are uniformly distributed with radial orientation, the expression of the potential is

$$V(\rho,z)=-\frac{v}{2\pi\varepsilon_0}\frac{1}{r_1}\left(J_1(k)+\frac{a^2-\rho^2-z^2}{(a-\rho)^2+z^2}J_2(k)\right)$$

where $J_1(k)$ is the complete elliptic integral of the first kind. On the axis of revolution the expression reduces to

$$V(0,z)=-\frac{va^2}{2\varepsilon_0}\frac{1}{r_1^3}.$$

The general case of arbitrary orientation can be computed by appropriate superposition.

References

Algora C, Sancho M, Martínez G (1987) Drift-diffusion model for absorption and resorption currents in polymers. J Appl Phys 61:4571–4578

Andersen OA (1983) Ion movement through gramicidin A channels. Interfacial Polarization effects on single-channel current measurements. Biophys J 41:135–146

Andersen OA, Koeppe RE II, Durkin JT, Mazet JL (1987) Structure-function studies on linear gramicidins: site-specific modifications in a membrane channel. In: Ion transport through membranes. Academic Press, New York. pp 295–314

Barrett EW, Weiss LB, Naveta FI, Koeppe RE II, Andersen OS (1986) Single-channel studies on linear gramicidins with altered amino acid side chains. Biophys J 49:673–686

Becker MD, Greathouse DV, Koeppe RE II, Andersen OA (1991) Amino acid sequence modulation of gramicidin channel function: Effects of tryptophan-to-phenylalanine substitutions on the single-channel conductance and duration. Biochemistry 30:8830–8839

Boni LT, Connolly AJ, Kleinfeld AM (1986) Transmembrane distribution of gramicidin by tryptophan energy transfer. Biophys J 49:122–123

Durand (1966) Electrostatique I. Masson, Paris, pp 183–186

Fonseca V, Daumas P, Ranjalahy-Rasoloarijao L et al. (1992) Gramicidin channels that have no tryptophan residues. Biochemistry 31:5340–5350

Gates P, Cooper K, Rae J, Eisenberg R (1989) Predictions of diffusion models for one-ion membrane channels. Prog Biophys Molec Biol 53:153–196

Harrington RF (1968) Field computation by moment methods. Macmillan, New York

Heitz F, Spach G, Trudelle Y (1982) Single channels of 9, 11, 13, 15-Destryptophyl-Phenilalanyl-Gramicidin A. Biophys J 40:87–89

Jordan PC (1981) Energy barriers for the passage of ions through channels. Exact solution of two electrostatic problems. Biophys Chem 13:203–212

Jordan PC (1982) Electrostatic modeling of ion pores. Energy barriers and electric field profiles. Biophys J 39:157–164

Jordan PC (1986) Ion channel electrostatics and the shapes of channel proteins. In: Miller C (ed) Ion channel reconstitution. Plenum Press, New York, pp 37–55

Jordan PC (1990) Ion-water and ion-polypeptide correlations in a gramicidin-like channel. Biophys J 58:1133–1156

Jordan PC, Bacquet RJ, McCammon JA, Tran P (1989) How electrolyte shielding influences the electrical potential in transmembrane ion channels. Biophys J 55:1041–1052

Koeppe RE II, Mazet JL, Andersen OS (1990) Distinction between dipolar and inductive effects in modulating the conductance of gramicidin channels. Biochemistry 29:512–520

Levitt DG (1978) Electrostatic Calculations for an ion channel. I. Energy and potential profiles and interactions between ions. Biophys J 22:209–219

Levitt DG (1986) Interpretation of biological ion channel flux data. Reaction-rate versus continuum theory. Annu Rev Biophys Chem 15:29–57

Martínez G, Sancho M (1990) Computer programs for the analysis of electrostatic potentials and electron trajectories. Nucl Instrum Methods A 298:70–77

Martínez G, Sancho M (1991) Application of the integral equation method to the analysis of electrostatic potentials and electron trajectories. In: Hawkes P (ed) Advances in electronics and electron physics, vol. 81. Academic Press, New York, pp 1–41

Monoi H (1991) Effective pore radius of the gramicidin channel. Biophys J 59:786–794

Partenskii MB, Jordan PC (1992) Nonlinear dielectric behavior of water in transmembrane ion channels: Ion energy barriers and the channel dielectric constant. J Phys Chem 96:3906–3910

Partenskii MB, Cai M, Jordan PC (1991) A dipolar chain model for the electrostatics of transmembrane ion channels. Chem Phys 153:125–131

Sancho M, Martínez G (1991) Electrostatic modeling of dipole-ion interactions in gramicidinlike channels. Biophys J 60:81–88

Warwicker J, Watson HC (1982) Calculation of the electric potential in the size cleft due to α-helix dipoles. J Mol Biol 157:671–679